GROUND-WATER FLOW AND SOLUTE MOVEMENT TO DRAIN LATERALS, WESTERN SAN JOAQUIN VALLEY, CALIFORNIA

II. QUANTITATIVE HYDROLOGIC ASSESSMENT

U.S. GEOLOGICAL SURVEY

Open-File Report 90-137

REGIONAL AQUIFER-SYSTEM ANALYSIS

Prepared in cooperation with the
SAN JOAQUIN VALLEY DRAINAGE PROGRAM

This report was prepared by the U.S. Geological Survey in cooperation with the San Joaquin Valley Drainage Program and as part of the Regional Aquifer-System Analysis (RASA) Program of the U.S. Geological Survey.

The San Joaquin Valley Drainage Program was established in mid-1984 and is a cooperative effort of the U.S. Bureau of Reclamation, U.S. Fish and Wildlife Service, U.S. Geological Survey, California Department of Fish and Game, and California Department of Water Resources. The purposes of the program are to investigate the problems associated with the drainage of agricultural lands in the San Joaquin Valley and to develop solutions to those problems. Consistent with these purposes, program objectives address the following key concerns: (1) public health, (2) surface- and ground-water resources, (3) agricultural productivity, and (4) fish and wildlife resources.

Inquiries concerning the San Joaquin Valley Drainage Program may be directed to:

San Joaquin Valley Drainage Program
Federal-State Interagency Study Team
2800 Cottage Way, Room W-2143
Sacramento, California 95825-1898

The RASA Program of the U.S. Geological Survey was started in 1978 following a congressional mandate to develop quantitative appraisals of the major ground-water systems of the United States. The RASA Program represents a systematic effort to study a number of the Nation's most important aquifer systems, which in aggregate underlie much of the country and which represent an important component of the Nation's total water supply. In general, the boundaries of these studies are identified by the hydrologic extent of each system, and accordingly transcend the political subdivisions to which investigations were often arbitrarily limited in the past. The broad objectives for each study are to assemble geologic, hydrologic, and geochemical information, to analyze and develop an understanding of the system, and to develop predictive capabilities that will contribute to the effective management of the system. The Central Valley RASA study, which focused on the hydrology and geochemistry of ground water in the Central Valley of California, began in 1979. Phase II of the Central Valley RASA began in 1984 and is in progress. The focus during this second phase is on more detailed study of the hydrology and geochemistry of ground water in the San Joaquin Valley, which is the southern half of the Central Valley.

GROUND-WATER FLOW AND SOLUTE MOVEMENT TO DRAIN LATERALS, WESTERN SAN JOAQUIN VALLEY, CALIFORNIA

II. QUANTITATIVE HYDROLOGIC ASSESSMENT

By *John L. Fio* and *S.J. Deverel*

U.S. GEOLOGICAL SURVEY

Open-File Report 90-137

REGIONAL AQUIFER-SYSTEM ANALYSIS

Prepared in cooperation with the
SAN JOAQUIN VALLEY DRAINAGE PROGRAM

Sacramento, California
1990

DEPARTMENT OF THE INTERIOR

MANUEL LUJAN, JR., *Secretary*

U.S. GEOLOGICAL SURVEY

Dallas L. Peck, *Director*

For additional information write to:

District Chief
U.S. Geological Survey
Federal Building, Room W-2234
2800 Cottage Way
Sacramento, CA 95825

Copies of this report may be purchased from:

U.S. Geological Survey
Books and Open-File Reports Section
Box 25425
Building 810, Federal Center
Denver, CO 80225

CONTENTS

ILLUSTRATIONS

TABLES

CONVERSION FACTORS

For use of readers who prefer inch-pound units, conversion factors for terms used in this report are listed below:

Multiply	By	To obtain
cubic meter per year (m^3/yr)	35.31	cubic foot per year
cubic meter per year per meter [$(m^3/yr)/m$]	10.76	cubic foot per year per foot
kilogram per year per meter [(kg/yr)/m]	0.00034	ton per year per foot
kilometer (km)	0.6214	mile
meter (m)	3.281	foot
meter per year (m/yr)	3.281	foot per year
square meter (m^2)	0.0002471	acre
square meter per year (m^2/yr)	0.0002471	acre per year
square meter per year per meter [$(m^2/yr)/m$]	3.281	square foot per year per foot

Sea Level: In this report, "sea level" refers to the National Geodetic Vertical Datum of 1929 (NGVD of 1929)—a geodetic datum derived from a general adjustment of the first-order level nets of both the United States and Canada, formerly called Sea Level Datum of 1929.

GROUND-WATER FLOW AND SOLUTE MOVEMENT TO DRAIN LATERALS, WESTERN SAN JOAQUIN VALLEY, CALIFORNIA

II. QUANTITATIVE HYDROLOGIC ASSESSMENT

By *John L. Fio* and *S.J. Deverel*

ABSTRACT

Ground-water-flow modeling was used to estimate ground-water-flow paths and traveltimes to quantitatively assess the hydrologic processes affecting ground water and solute movement to drain laterals. Modeling results were used to calculate the depth distribution of ground water flowing into drain laterals at 1.8 meters (drain lateral 1) and 2.7 meters (drain lateral 2) below land surface. The simulations indicated that under nonirrigated conditions about 89 percent of the flow in drain lateral 2 was from ground water originating from depths greater than 6 meters below land surface. The deep ground water has higher selenium concentrations than shallow ground water. Simulation of irrigated conditions indicates that as recharge increases, the proportion of deep ground water entering the drain laterals decreases.

Ground-water-flow modeling also was used to estimate selenium loads in drain laterals for varying drain-lateral flow rates. Simulated loads are in general agreement with measured loads and increase with increasing drain-lateral flow. Simulations further indicate ground water that contains high-selenium concentrations probably will continue to enter drain lateral 2 for more than 8 years.

INTRODUCTION

Subsurface drainage systems were installed in some agricultural areas of the western San Joaquin Valley, California, where a shallow water table and saline ground water became detrimental to crop production. Many of these drainage systems collect ground water that was enriched in salinity and selenium by evapotranspiration prior to drainage-system installation (Deverel and Fujii, 1988; Deverel and Gallanthine, 1989). Since the drainage systems were installed, the saline and high-selenium ground water is being displaced downward and toward the drain laterals by less saline irrigation recharge.

Previous reports on the quantitative assessment of ground-water flow and solute transport to drain laterals assumed the existence of an impermeable layer at some depth below the drain laterals (Kirkham, 1949, 1958; Luthin and others, 1969; Ortiz and Luthin, 1970; Jury 1975a, 1975b; and Pickens and others, 1979). For conditions of uniform recharge to the water table, this approach predicts concentric flow paths extending from midway between two drain laterals to the drain lateral. For the geohydrologic conditions in the San Joaquin Valley, traveltime for ground water moving along the deepest flow paths can be as long as 50 years (Jury, 1975b). The composition of the resulting drain water is dependent, therefore, on the interception and mixing of relatively older ground water flowing along deep flow paths and more recently recharged ground water flowing along the shallow flow paths.

In a companion paper, Deverel and Fio (1990) analyzed geochemical and hydrologic data in a drained agricultural field in the western San Joaquin Valley. They showed that the chemical and isotopic composition of drain-lateral water is the result of mixing of deep (greater than 6 m below land surface) and shallow (less than 6 m below land surface) ground water. The deeper water was near land surface in the past and was enriched in oxygen-18 and deuterium by evapotranspiration prior to installation of the drainage system. Salinity and selenium concentrations are higher in this older water relative to the shallow ground water recharged from recent irrigations. Deverel and Fio (1990) used the different isotopic compositions of the shallow and deep ground water to calculate the proportions of each entering drain laterals at 1.8 and 2.7 m below land surface. More deep ground water enters the drain lateral at the 2.7-meter depth, and consequently the annual selenium load from this drain lateral is more than four times the annual selenium load from the drain lateral at the 1.8-meter depth.

This paper describes results of a quantitative assessment of ground-water flow and advective solute movement under steady-state conditions in a drained agricultural field described by Deverel and Fio (1990). The objectives of the study were to further quantify the concepts and calculations discussed in Deverel and Fio (1990) and to evaluate the effects of recharge rate and drain-lateral depth on selenium concentrations and loads in drain-lateral water. This study is part of a comprehensive investigation of the hydrology and geochemistry of the San Joaquin Valley by the U.S. Geological Survey. The studies are being done in cooperation with the San Joaquin Valley Drainage Program and as part of the Regional Aquifer-System Analysis Program of the U.S. Geological Survey.

APPROACH

A steady-state, finite-difference, two-dimensional ground-water-flow model was used to simulate hydrologic conditions in the geohydrologic section A-A' (Deverel and Fio, 1990, fig. 2). The use of the finite-difference model was necessary to adequately assess ground-water flow because of the nonhomogeneous geology and the influence of regional hydraulic gradients on ground-water flow in the section. Ground-water-flow paths and traveltimes in the section were calculated from the flow model results using the program Modpath (Pollock, 1989) to simulate advective solute movement to drain laterals. The modeling results were used with geochemical data from ground-water samples to estimate selenium loads from the drain laterals.

A steady-state modeling approach was used to estimate annual ground-water-flow characteristics that change between irrigated and nonirrigated conditions during the year. Ground-water characteristics of the shallow flow system associated with drainage systems in the western San Joaquin Valley are typically steady and show small seasonal variation (Belitz and Heimes, 1990). The ground-water-flow model was developed and calibrated for the average flow characteristics measured in the field during October 1987 to November 1988 when the field was idle and did not receive irrigation recharge (nonirrigated conditions). Recharge then was included in the model to simulate average flow characteristics measured during January 1987 to January 1988 when the field received periodic applications of irrigation water (irrigated conditions). Transient characteristics of annual ground-water flow in the field are a combination of the conditions represented by the irrigated and nonirrigated simulations. The ground-water-flow model results were used to estimate average ground-water flow and advective solute movement from different depths to the drain laterals and to evaluate the effects of annual recharge rate on flow and selenium loads in the drain laterals. Geochemical and hydrologic data presented by Deverel and Fio (1990) were used to verify the results of the ground-water-flow simulations.

METHOD USED TO MODEL GROUND-WATER FLOW

GOVERNING EQUATION

A numerical, finite-difference ground-water-flow model (McDonald and Harbaugh, 1988) was used to simulate the distribution of hydraulic heads in the section and volumetric fluxes to the drain laterals. Steady-state, three-dimensional movement of ground water of constant density through porous earth material is described by the partial-differential equation:

$$\partial/\partial X\,(K_{xx}\,\partial h/\partial X) + \partial/\partial Y\,(K_{yy}\,\partial h/\partial Y) + \partial/\partial Z\,(K_{zz}\,\partial h/\partial Z) - W = 0 \quad (1)$$

where

K_{xx}, K_{yy}, K_{zz} are values of the hydraulic conductivity along the x, y, and z coordinate axis, which are assumed to be parallel to the major axes of hydraulic conductivity, in meters per year;

h is the hydraulic head, in meters; and

W is a volumetric flux per unit volume and represents sources and/or sinks of water, in year $^{-1}$.

Equation 1 describes ground-water flow in a heterogeneous and anisotropic medium. Using a right-hand coordinate system, application of the three-dimensional equation to the geohydrologic section requires the reduction of the x-y-z cartesian coordinate system to a x-z coordinate system (McDonald and Harbaugh, 1988). Specifications of flow and/or head conditions at the boundaries of the model constitute a mathematical representation of the ground-water-flow system and when solved provide the hydraulic head distribution over the x-z space.

FINITE-DIFFERENCE GRID

An approximate solution of the ground-water-flow equation 1 was obtained using the finite-difference method where the continuous system described by

equation 1 was replaced by a finite set of discrete points in space (McDonald and Harbaugh, 1988). The model is discretized into a grid of finite-difference cells and simulated as a vertical plane of unit depth in the *y* direction with no flow orthogonal to the *x*-*z* plane. Solving the set of finite-difference equations results in head values for each finite-difference cell.

The finite-difference grid (fig. 1) consists of 26 layers (each 1 m thick) and 169 columns of variable widths. The water table is about 1.5 m below land surface and is represented in the top model layer. The uppermost eight layers of finite-difference cells represent clay loam. The remaining 18 layers represent underlying sand (Deverel and Fio, 1990). The geohydrologic section A-A' is represented by the central part of the finite-difference grid and consists of 145 square cells of constant width (1 m). The influence of the boundary conditions of the ground-water-flow model are minimized by extending the lateral boundaries of the finite-difference grid about 200 m beyond the boundaries of the section. The additional finite-difference cells were of variable widths, and the ratio of adjacent cell widths was maintained less than 1.5 to avoid truncation errors and possible convergence problems as suggested by Trescott and others (1976).

BOUNDARY CONDITIONS

Four types of boundary conditions were used in the model: (1) a water table or free-surface boundary, (2) a no-flow boundary, (3) a specified flow (Neumann) boundary, and (4) a head-dependent flow (Cauchy) boundary (McDonald and Harbaugh, 1988). Figure 2 shows the boundary conditions used in the ground-water-flow model. The water table near the top of the section was represented as a free-surface boundary, and the model simulated a net recharge to the water table from irrigation across this boundary. A no-flow boundary in the sand layer at the bottom of the section was used to represent the horizontal flow path near that depth (Deverel and Fio, 1990). Because the model does not simulate upward movement of ground water across the no-flow boundary, horizontal flow is considered the principal contribution of ground water to the section from sources outside the model boundaries.

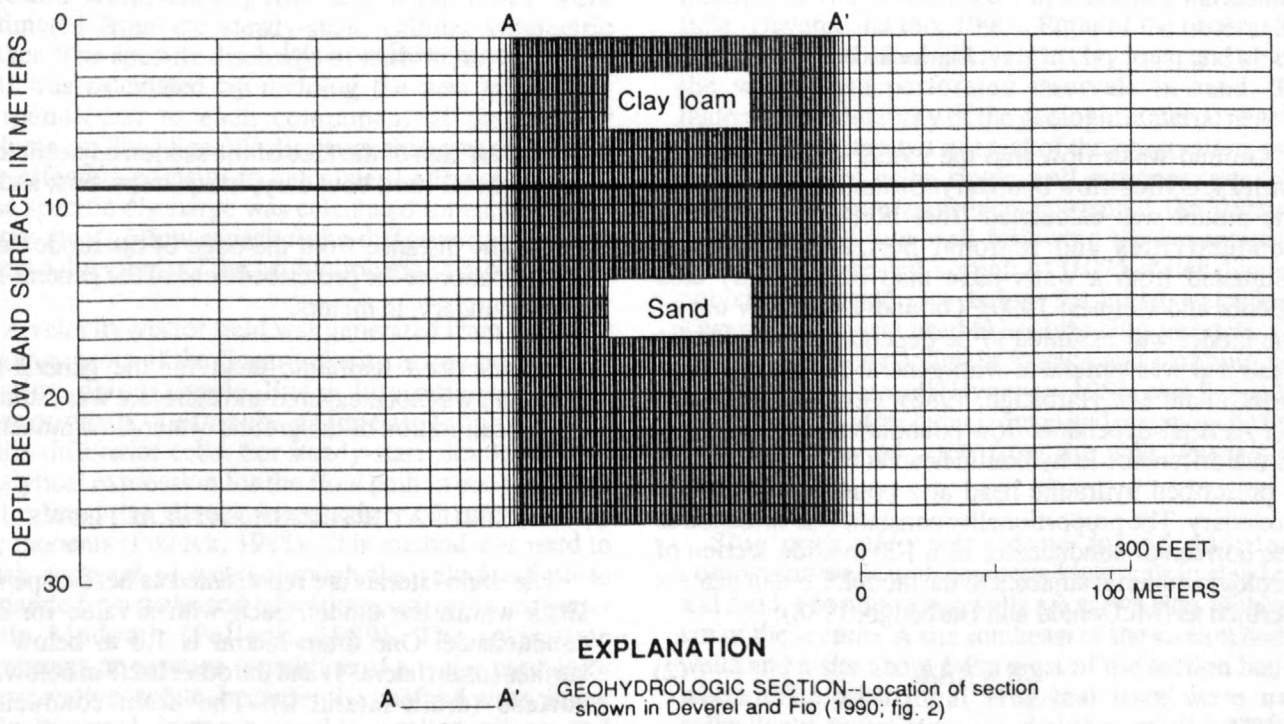

Figure 1. Finite-difference grid and geologic framework for ground-water-flow model of geohydrologic section A-A'.

and detector was done with aluminum tubes (0.04 m in diameter) installed to a depth of 1.5 m at each of the four cluster sites (Deverel and Fio, 1990, fig. 2). Gravimetric measurement of the moisture content of soil samples collected during access tube installation was used for calibration. The total soil porosity was estimated by the saturated water content measured immediately after irrigation. The effective soil porosity or specific yield was estimated from the difference between the saturated water content and the water content after drainage.

DEVELOPMENT OF GROUND-WATER-FLOW MODEL

For simulation of ground-water flow in the geohydrologic section during nonirrigated conditions, the model required specification of drain conductance, horizontal and vertical hydraulic conductivity, ground-water flow into the section from the specified flow boundary, and ground-water flow out of the section through the head-dependent flow boundary. Most of the input to the ground-water-flow model for simulation of the nonirrigated conditions was determined from data collected in the field.

Drain conductance was estimated from drain-lateral flows measured in drain lateral 2 and the difference in hydraulic head between the drain lateral and an observation well near the drain. Figure 3 shows the relation of drain-lateral flow and the hydraulic-head difference. The data do not fall on a unique line and are dependent on hydrologic conditions. Most of the points in figure 3 represent data that were collected when the water table intersected the drain lateral and the soil profile above the drain lateral was unsaturated (nonirrigated conditions). Under these conditions, ground-water flow to the drain lateral generally is from areas adjacent to and beneath the drain lateral. The slope of the line determined from least-squares regression for the nonirrigated conditions is 100 (m^2/yr)/m.

The second group of data associated with an irrigation in November 1988 does not plot on a single regression line. Much of the drain-lateral water during the irrigated conditions probably flowed from flow paths originating within meters of the drain lateral (Luthin and others, 1969; Ortiz and Luthin, 1970). The installation of drain laterals disrupts the soil and results in the formation of a "trench" of more permeable soil overlying the drain laterals. During irrigation, large quantities of water applied at land surface can flow through this trench to a drain lateral (Tod and Grismer, 1988). The slope of the

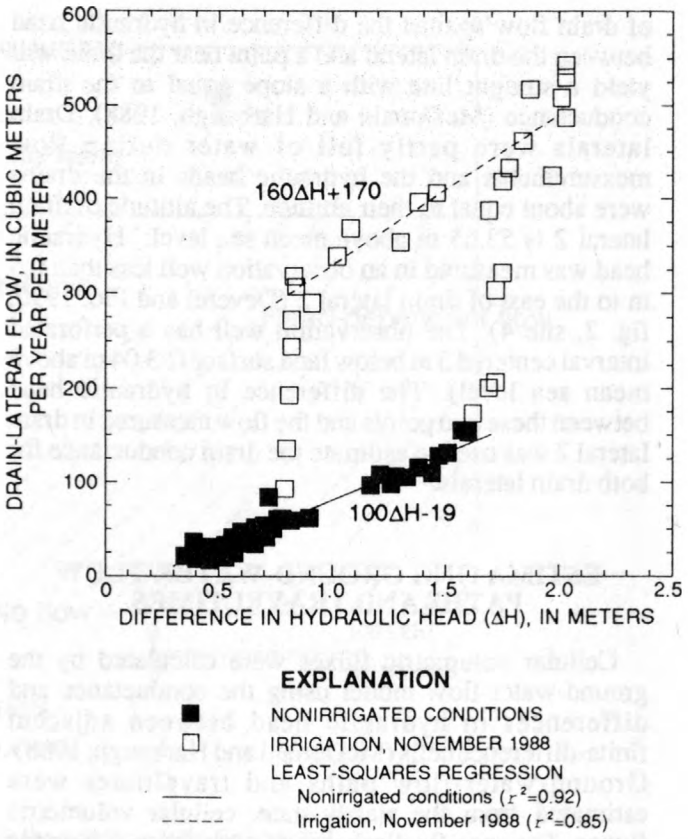

Figure 3. Relation of drain-lateral flow and the difference in hydraulic head between the 3-meter well at site 4 and the drain lateral.

regression line for the irrigation in November 1988 is 160 (m^2/yr)/m (fig. 3). High flows caused by irrigation persisted in drain lateral 2 for several days after irrigation water no longer was ponded over drain lateral 2 (Deverel and Fio, 1990), however, drain conductance for drain lateral 2 returned to levels characteristic of nonirrigated conditions about 6 hours after the application of irrigation water to areas above this drain lateral was ended. Because the flow model was calibrated to the nonirrigated conditions, the value of 100 (m^2/yr)/m was used for drain conductance. Additional ground-water-flow simulations were done to assess the sensitivity of model results to drain conductance.

Hydraulic conductivities for the clay loam and sand in the section were estimated from slug-test results summarized in table 1. The hydraulic conductivities from the slug-test results are lognormally distributed. The geometric means of the hydraulic conductivities

Table 1. Summary of geometric means and innerquartile range (in parentheses) for values of hydraulic conductivity for clay loam and sand aquifer materials from analysis of the slug-test results by the methods of Hvorslev (1951) and Cooper and others (1967)

Texture	Number of wells	Hydraulic conductivity (m/yr)	
		Hvorslev method	Cooper and others method
Clay loam	65	270 (116, 577)	670 (310, 1,580)
Sand	15	1,200 (524, 4,607)	2,300 (630, 11,600)

determined by the method of analysis described by Cooper and others (1967) were 670 and 2,300 m/yr for the clay loam and sand, respectively. This method of analyzing slug-test data assumes horizontal flow from a fully penetrating well. During the slug test if vertical flow occurs near the partly penetrating wells, these hydraulic conductivities probably will be larger than the actual values. The method of analysis described by Hvorslev (1951) assumes isotropic flow of water from the observation well but neglects specific storage. The geometric means of the hydraulic conductivities determined by the method of analysis described by Hvorslev (1951) were 270 and 1,200 m/yr for clay loam and sand, respectively, and are smaller than the values from the method described by Cooper and others (1967). We used initial estimates of 670 and 2,300 m/yr for the horizontal hydraulic conductivity of the clay loam and sand, respectively. Additional ground-water-flow simulations were done to assess the sensitivity of model results to hydraulic conductivity.

Horizontal and vertical hydraulic conductivities in the section probably are not equal. The median horizontal to vertical permeability ratios measured in clay loam and sand deposits from well cores taken from the central part of the western San Joaquin Valley were 3:1 and 2:1, respectively (Johnson and others, 1968). Results from the two slug-test analyses and stratification evident in well cores sampled during this study were used to qualitatively estimate a horizontal to vertical ratio of hydraulic conductivity in the clay loam and sand of 6:1 and 4:1, respectively. Additional ground-water-flow simulations were done to assess the sensitivity of model results to the ratio of horizontal to vertical hydraulic conductivity.

Ground-water flow into the section from the specified-flow boundary was determined from horizontal hydraulic conductivity and the regional horizontal gradient. The component of the regional horizontal gradient in the direction of the section is about 0.0015 (Belitz and Heimes, 1990). The contribution of regional ground-water flow to the model therefore is about 70 m^3/yr. The external head at the general-head boundary was adjusted to estimate ground-water flow out of the model and match the drain flow and hydraulic-head gradients measured in the section during the study. The irrigated conditions were simulated with the calibrated model by including net recharge to the water table.

SIMULATION OF NONIRRIGATED GROUND-WATER-FLOW CONDITIONS

The distribution of hydraulic heads during nonirrigated conditions was simulated using an exterior head at the general-head boundary of 54.14 m. In drain laterals 1 and 2, the model simulated nonirrigated flow rates of 4 and 46 (m^3/yr)/m of drain lateral. These flow rates are in general agreement with the median values measured during the nonirrigated period (10 and 30 (m^3/yr)/m of drain lateral, respectively). The model estimates a flow rate of about 39 m^3/yr for ground water moving beyond the boundary of the section. Ground water flowing out of the section is intercepted downslope by other drain laterals or moves past the boundaries of the field with the regional ground-water-flow system. An exterior head at the general-head boundary that is larger than 54.14 m results in less flow out of the section and smaller hydraulic gradients than measured during the study. An exterior head that is smaller than 54.14 m results in more flow out of the section and hydraulic gradients that are larger than measured during the study.

The measured and simulated distribution of hydraulic heads for the nonirrigated conditions is shown in figure 4. The hydraulic heads measured in observation wells at sites 1 and 2 (Deverel and Fio, 1990, fig. 2) are projected onto the section. Figure 4 shows large hydraulic-head gradients near drain lateral 2, but more

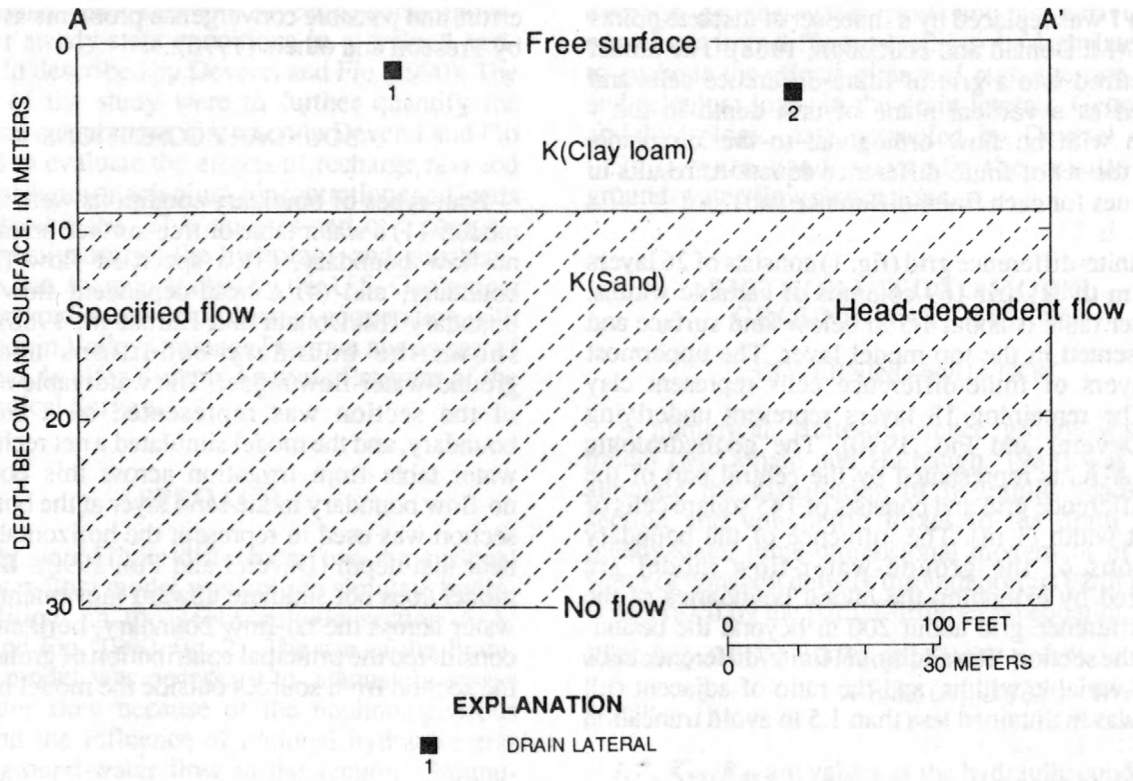

Figure 2. Boundary conditions for the ground-water-flow model.

Ground-water flow into the model was represented with a specified-flow boundary. Ground-water flow into the model was calculated from horizontal hydraulic conductivities and regional horizontal gradients estimated from a water-table map of the study area (Belitz and Heimes, 1990). Ground-water flow out of the model was assumed to be dependent on hydraulic head and was simulated with general-head boundaries (McDonald and Harbaugh, 1988). Ground-water flow across head-dependent flow boundaries is proportional to the difference in hydraulic head at the boundary and a prescribed hydraulic head at a point exterior to the boundary. The proportionality constant was specified as the horizontal conductance of a 100 m wide section of geologic material adjacent to the model. Conductance is defined as (McDonald and Harbaugh, 1988):

$$CB = KA/L \qquad (2)$$

where

CB is the conductance, in square meters per year;

K is the horizontal hydraulic conductivity of the geologic material adjacent to the model, in meters per year;

A is the area of the face of the section adjacent to the general-head boundary, in square meters; and

L is the distance from the edge of the model to the location of the prescribed head of the general-head boundary, in meters.

The prescribed hydraulic head for the general-head boundary was not measured and therefore was estimated during calibration of the ground-water-flow model.

SIMULATING DRAIN-LATERAL FLOWS

The drain laterals are represented as head-dependent sinks within the model, each with a value for drain conductance. One drain lateral is 1.8 m below land surface (drain lateral 1) and the other is 2.7 m below land surface (drain lateral 2). The drain conductance accounts for the combined effects of head losses associated with convergence of flow at the drain lateral, differences in hydraulic conductivity of materials immediately around the drain lateral, and flow through the wall of the drain lateral (McDonald and Harbaugh, 1988). A linear function is used to describe drain-lateral flows. The use of a linear function assumes that a plot

of drain flow against the difference in hydraulic head between the drain lateral and a point near the drain will yield a straight line with a slope equal to the drain conductance (McDonald and Harbaugh, 1988). Drain laterals were partly full of water during flow measurements and the hydraulic heads in the drains were about equal to their altitude. The altitude of drain lateral 2 is 53.65 m above mean sea level. Hydraulic head was measured in an observation well less than 0.5 m to the east of drain lateral 2 (Deverel and Fio, 1990, fig. 2, site 4). The observation well has a perforated interval centered 3 m below land surface (53.04 m above mean sea level). The difference in hydraulic head between these two points and the flow measured in drain lateral 2 was used to estimate the drain conductance for both drain laterals.

ESTIMATING GROUND-WATER-FLOW PATHS AND TRAVELTIMES

Cellular volumetric fluxes were calculated by the ground-water-flow model using the conductance and differences in hydraulic head between adjacent finite-difference cells (McDonald and Harbaugh, 1988). Ground-water-flow paths and traveltimes were estimated from the steady-state, cellular volumetric fluxes. The specific discharge of each finite-difference cell was calculated by dividing the area of the cell perpendicular to each component of the cellular volumetric flux. Specific discharge then was divided by the effective porosity to calculate the linear velocity. The specific discharge was calculated for each cellular component of flow at each finite-difference node in the x and z directions of the geohydrologic section.

A velocity-vector field was generated from the x and z components of the linear velocity at any point in the section using simple linear interpolation of the components between adjacent faces of the finite-difference cells. For steady-state simulations, an analytical expression for the flow path in each cell was calculated by direct integration of the velocity components (Pollock, 1988). This method was used to track a packet of water through the velocity field to generate flow paths and traveltimes using the computer code Modpath (Pollock, 1989). The traveltime represents an average traveltime of a water particle or conservative solute because the method uses linear velocities and does not consider scaling effects and dispersive mechanisms that substantially can reduce the advective movement of ground water and solutes (Reilly and others, 1987).

Ground-water flow in stream tubes defined by the region between two adjacent flow paths was calculated from flow-model results. The stream tubes converging at the drain lateral were delineated as originating at depths greater than 6 m from land surface (below the drain laterals) or from depths adjacent to and above the drain laterals. Ground water in the section at depths greater than 6 m generally is older and enriched in oxygen-18 and selenium relative to the more recent irrigation recharge from depths above and adjacent to the drain laterals (Deverel and Fio, 1990). Specific discharge of ground water to the drain lateral was assumed to be constant over each face of the finite-difference cell containing the drain lateral. The fraction of discharge in each stream tube therefore was directly proportional to the area between two stream tubes intersecting a face of the finite-difference cell. This approach was used to quantify the proportion of simulated ground-water flow entering the drain laterals from different depths in the section.

FIELD METHODS USED TO DETERMINE HYDRAULIC CONDUCTIVITYAND EFFECTIVE POROSITY

Observation wells (0.05-meter diameter) were installed at four cluster sites in a drained agricultural field (Deverel and Fio, 1990). Eight of the observation wells have perforated intervals in clay loam and nine of the wells have perforated intervals in sand. The hydraulic conductivity of the geologic material near the 0.61-meter perforated interval of the observation wells was determined using single-well response tests (slug tests). A pressure transducer measured the decay of hydraulic head in a well following the instantaneous insertion of a sealed section of 0.025-meter diameter polyvinyl-chloride pipe below the initial water level. Two methods were used to analyze slug-test data. One method assumes negligible storage and isotropic flow of water from the well (Hvorslev, 1951, case 8, fig. 12); the other method includes storage and assumes confined horizontal flow of water from the well (Cooper and others, 1967).

Slug tests also were done for 65 additional observation wells with perforated intervals in clay loam and sand. The additional wells are at two sites within 30 km of the section. A site southeast of the section had 51 wells and a site about 5 km west of the section had 14 wells. The additional slug-test data were used collectively to estimate the distribution of hydraulic conductivity for clay loam and sand deposits in the study area and in the section.

The total and effective soil porosity of the top 1.5 m of surface material were measured using the neutron method (Bouwer, 1978). Access of the neutron source

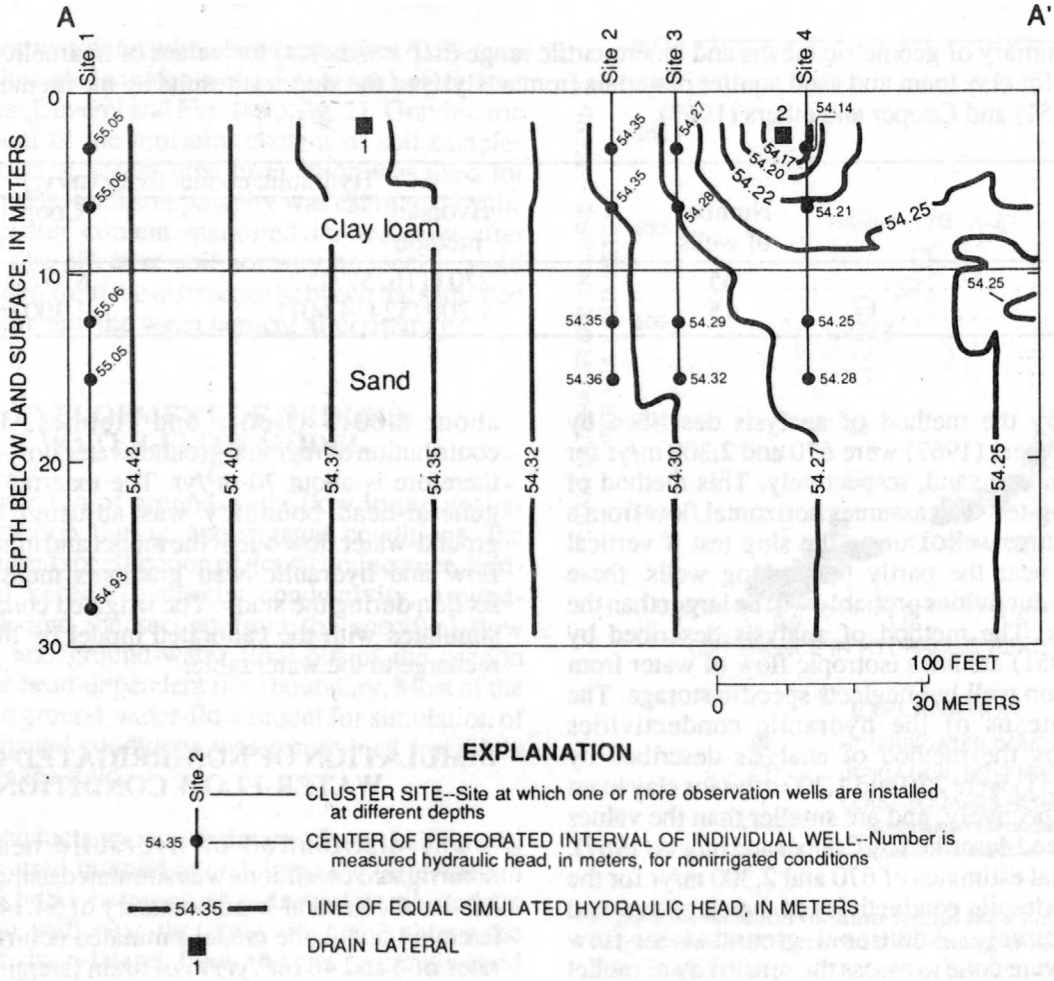

Figure 4. Distribution of measured and simulated hydraulic heads for nonirrigated conditions. Simulated flow for drain lateral 1 is 4 $(m^3/yr)/m$; drain lateral 2 is 46 $(m^3/yr)/m$.

flow occurs in the sand because of its larger hydraulic conductivity. The distribution of hydraulic head is not symmetric around the drain laterals because ground-water flow to the drain laterals is affected by regional gradients. The model results indicate that hydraulic gradients downgradient of drain lateral 2 are low and that there is an area of stagnation. Ground-water flow around the stagnation point divides the ground-water-flow system into water that is intercepted by the drain laterals and ground water that flows downgradient past the drains.

Ground-water-flow paths and estimated traveltimes for nonirrigated conditions are shown in figure 5. Ground-water flow generally is horizontal except where affected by drain laterals. The model results indicate that ground water in the sand layer flows upward to drain lateral 2 but not to drain lateral 1. The flow path at 21 m is the deepest flow path to be intercepted by the drain laterals. Deverel and Fio (1990) presented hydraulic-head data indicating that hydraulic-head gradients generally are upward from 15 m below land surface. Gradients reverse and are vertically downward somewhere between 15 and 27 m below land surface.

Estimated traveltimes for flow paths in figure 5 show that ground water at the upgradient boundary of the section when the drain laterals were installed (1969) requires between 8 and 34 years to reach drain lateral 2, resulting in arrival dates between 1977 to 2003. The traveltimes were estimated from linear velocities calculated from the effective porosity measured in the clay loam (0.1) and an assumed porosity of 0.3 for the sand. Ground water below drain lateral 1 and in the sand layer is flowing upwards and towards drain lateral 2. This flow path passes through the areas where the perforated

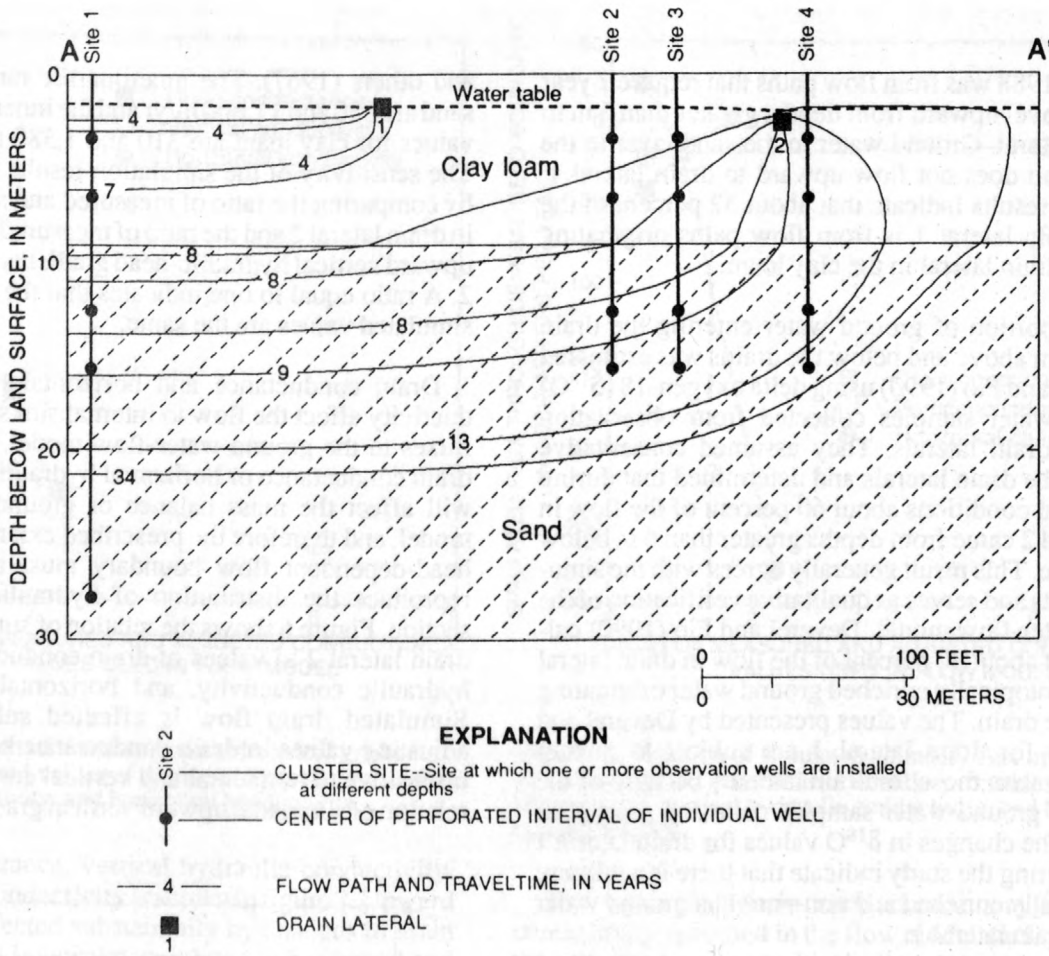

Figure 5. Simulated ground-water-flow paths and estimated traveltimes for nonirrigated conditions. Simulated flow for drain lateral 1 is 4 (m^3/yr)/m; drain lateral 2 is 46 (m^3/yr)/m.

intervals of the 3- and 6-meter wells at sites 2 and 3 are located. Deverel and Fio (1990) reported that the ground-water sample collected from the 6-meter well at site 2 in 1988 was more isotopically enriched than samples collected in 1987 (Deverel and Fio, 1990, fig. 8). The estimated traveltime of ground water to reach this sampling point from areas below the 6-meter depth and at the edge of the section is about 8 years after installation of the drain laterals (1977). The mean traveltime of dissolved constituents in ground water flowing to the drain laterals as indicated by the isotope data is about 10 years longer than estimated from the linear ground-water velocities of the nonirrigated simulation. Irrigation probably has altered the flow paths and dispersive mechanisms have affected the traveltime and chemical composition of ground water flowing to the drain laterals.

Summation of the ground-water flow in stream tubes defined by adjacent flow paths (fig. 5) indicated that about 89 percent of the flow in drain lateral 2 for nonirrigated conditions is ground water flowing from depths greater than 6 m below land surface. The field has received intermittent irrigations since installation of the drain laterals, and the annual flow paths and resulting depth distribution of chemical constituents near drain lateral 2 surely have been affected by the mixing of relatively high quality water from past irrigations with deep, low quality ground water that infiltrated prior to drainage-system installation. During the year that the field was not irrigated (1988), the actual contribution of flow to drain lateral 2 from ground water originating from depths greater than 6 m below land surface therefore probably was less than 89 percent. The model results indicate that about 69 percent of the flow in drain

lateral 2 in 1988 was from flow paths that require 1 year or less to travel upward from depths greater than 6 m to the drain lateral. Ground water in the sand layer in the A-A' section does not flow upward to drain lateral 1. The model results indicate that about 52 percent of the flow in drain lateral 1 is from flow paths originating below the drain lateral in the clay loam.

The proportion of ground water entering the drain laterals from above and below the drains was estimated by Deverel and Fio (1990) using delta oxygen-18 ($\delta^{18}O$) values of water samples collected from observation wells and drain laterals. They assumed conservative mixing in the drain laterals and determined that during nonirrigated conditions about 60 percent of the flow in drain lateral 2 came from depths greater than 6 m below land surface. This result generally agrees with the simulation results and serves as qualitative verification of the ground-water-flow model. Deverel and Fio (1990) calculated that about 30 percent of the flow in drain lateral 1 is from isotopically enriched ground water originating beneath the drain. The values presented by Deverel and Fio (1990) for drain lateral 1 are subject to greater uncertainty than those for drain lateral 2 because of the absence of ground-water samples collected near drain lateral 1. The changes in $\delta^{18}O$ values for drain lateral 1 samples during the study indicate that there is a mixture of isotopically enriched and non-enriched ground water entering drain lateral 1.

SENSITIVITY OF GROUND-WATER-FLOW MODEL TO DRAIN CONDUCTANCE AND HYDRAULIC CONDUCTIVITY

The sensitivity of ground-water flow to different values of drain conductance, vertical hydraulic conductivity, and horizontal hydraulic conductivity was evaluated with six additional nonirrigated-flow simulations. The first simulation used a drain conductance of 50 m^2/yr, and the second simulation used a value of 160 m^2/yr. The value of 160 m^2/yr was estimated from data collected during irrigation in November 1988 (fig. 3). The third and fourth simulations assessed the effect of vertical hydraulic conductivity on ground-water flow. The third simulation used equal horizontal and vertical conductivities (isotropic conditions), and the fourth simulation used vertical conductivities that were one-half of the values estimated with the slug-test data. The last two nonirrigated-flow simulations assessed the effect of horizontal hydraulic conductivity by using the innerquartile range of the distribution of hydraulic conductivity values from the method of analysis described by Cooper and others (1967). The innerquartile range values for sand are 630 and 11,600 m/yr and the innerquartile range values for clay loam are 310 and 1,580 m/yr (table 1). The sensitivity of the simulation results was evaluated by comparing the ratio of measured and simulated flow in drain lateral 2 and the ratio of measured and simulated upward vertical hydraulic-head gradients to drain lateral 2. A ratio equal to one indicates that the measured and simulated values are the same.

Drain conductance and horizontal hydraulic conductivity affect the flow to internal sinks and boundary fluxes in the ground-water-flow model. Adjusting the drain conductance or horizontal hydraulic conductivity will affect the mass balance of ground water in the model, and therefore the prescribed external head at the head-dependent flow boundary must be adjusted to reproduce the distribution of hydraulic head in the section. Figure 6 shows the relation of simulated flow in drain lateral 2 to values of drain conductance, vertical hydraulic conductivity, and horizontal conductivity. Simulated drain flow is affected substantially by adjusting values in drain conductance but is relatively insensitive to horizontal and vertical conductivity. The relation of simulated upward vertical gradients to values

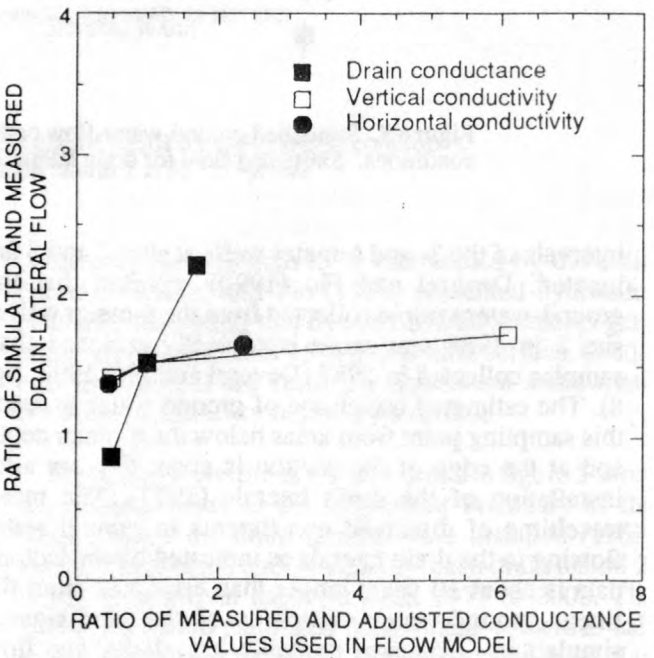

Figure 6. Relation of simulated flow in drain lateral 2 to values of drain conductance, vertical hydraulic conductivity, and horizontal conductivity.

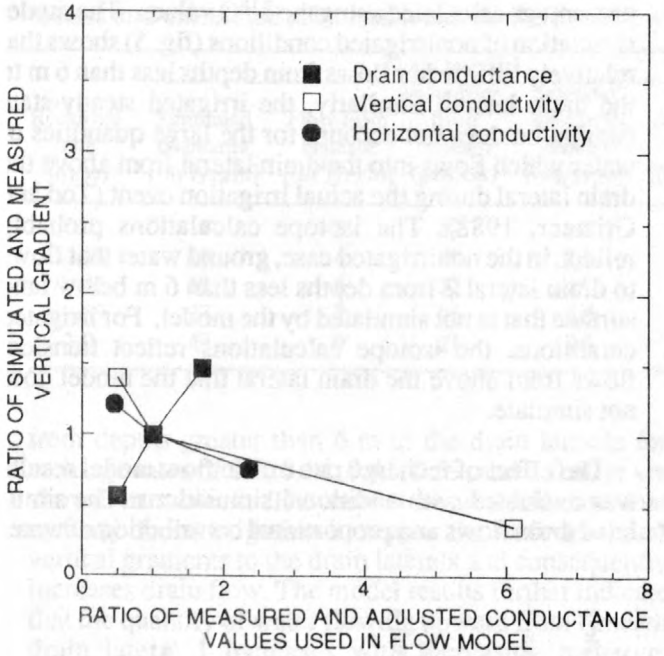

Figure 7. Relation of simulated upward vertical gradients to drain lateral 2 and values of drain conductance, vertical hydraulic conductivity, and horizontal conductivity.

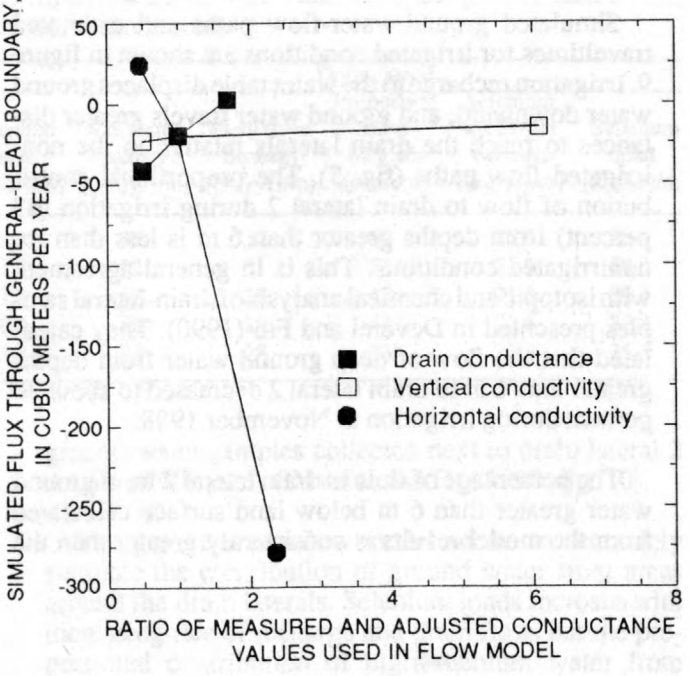

Figure 8. Relation of simulated boundary flux of ground water through the general-head boundary to values of drain conductance, vertical hydraulic conductivity, and horizontal conducitvity.

of drain conductance, vertical hydraulic conductivity, and horizontal conductivity is shown in figure 7. Upward gradients are affected substantially by changes in drain conductance and inversely are related to horizontal and vertical conductivity. The results shown in figures 6 and 7 indicate that improved simulation of the nonirrigated flow characteristics to drain lateral 2 can be accomplished by reducing drain conductance and vertical and/or horizontal hydraulic conductivity.

Adjustments to drain conductance and hydraulic conductivity substantially affect ground-water flow at the boundaries and the direction and shape of ground- water-flow paths in the section. Figure 8 shows the relation of simulated boundary flux of ground water through the general-head boundary to values of drain conductance, and vertical and horizontal hydraulic conductivities. An increase in drain conductance requires ground water to flow into the section from the head-dependent flow boundary. Low values of horizontal hydraulic conductivity affect the quantity of water entering the section from the specified-flow boundary and also require ground water to flow into the section from the head-dependent flow boundary. In the field, ground water probably does not flow to drain lateral 2 from the areas represented by the head-dependent flow boundary. The drain conductance therefore probably is smaller than 160 m^2/yr, and the horizontal conductivity in the clay loam and sand is greater than 310 and 630 m/yr, respectively.

The values of drain conductance and hydraulic conductivity specified in the flow model are higher than the apparent optimum values indicated by the sensitivity analysis. The existing flow model was considered adequate to describe nonirrigated-flow conditions in the section because the apparent optimum values did not significantly affect ground-water-flow paths and the proportional contribution of flow from beneath drain lateral 2. Recharge from irrigation was included in the model to study the effect of irrigation on ground-water flow to the drains.

SIMULATION OF IRRIGATED GROUND-WATER-FLOW CONDITIONS

Irrigated ground-water-flow conditions were simulated by including net recharge to the water table in the model. The recharge rate was estimated by increasing its value until the simulated distribution of hydraulic heads agreed with the values measured in the field under irrigated conditions. The measured irrigated flow characteristics in the geohydrologic section were reproduced using an annual rate of net recharge to the water table of 0.59 m/yr. The model results show flow rates in the drain laterals increase due to irrigation. The simulated flows in drain laterals 1 and 2 for the irrigated conditions were 27 and 68 (m^3/yr)/m.

Simulated ground-water-flow paths and estimated traveltimes for irrigated conditions are shown in figure 9. Irrigation recharge to the water table displaces ground water downward, and ground water travels greater distances to reach the drain laterals relative to the nonirrigated flow paths (fig. 5). The proportional contribution of flow to drain lateral 2 during irrigation (43 percent) from depths greater than 6 m is less than for nonirrigated conditions. This is in general agreement with isotopic and chemical analysis of drain-lateral samples presented in Deverel and Fio (1990). They calculated that the flow of deep ground water from depths greater than 6 m to drain lateral 2 decreased to about 30 percent during irrigation in November 1988.

The percentage of flow in drain lateral 2 from ground water greater than 6 m below land surface calculated from the model results is consistently greater than the percentage calculated using the $\delta^{18}O$ values. The model simulation of nonirrigated conditions (fig. 5) shows that relatively little water flows from depths less than 6 m to the drain lateral. Similarly, the irrigated steady-state simulation does not account for the large quantities of water which flows into the drain lateral from above the drain lateral during the actual irrigation event (Tod and Grismer, 1988). The isotope calculations probably reflect, in the nonirrigated case, ground water that flows to drain lateral 2 from depths less than 6 m below land surface that is not simulated by the model. For irrigated conditions, the isotope calculations reflect transient flows from above the drain lateral that the model does not simulate.

The effect of recharge rate on the flow model results was evaluated with additional simulations. The simulated drain flows and proportional contribution of water

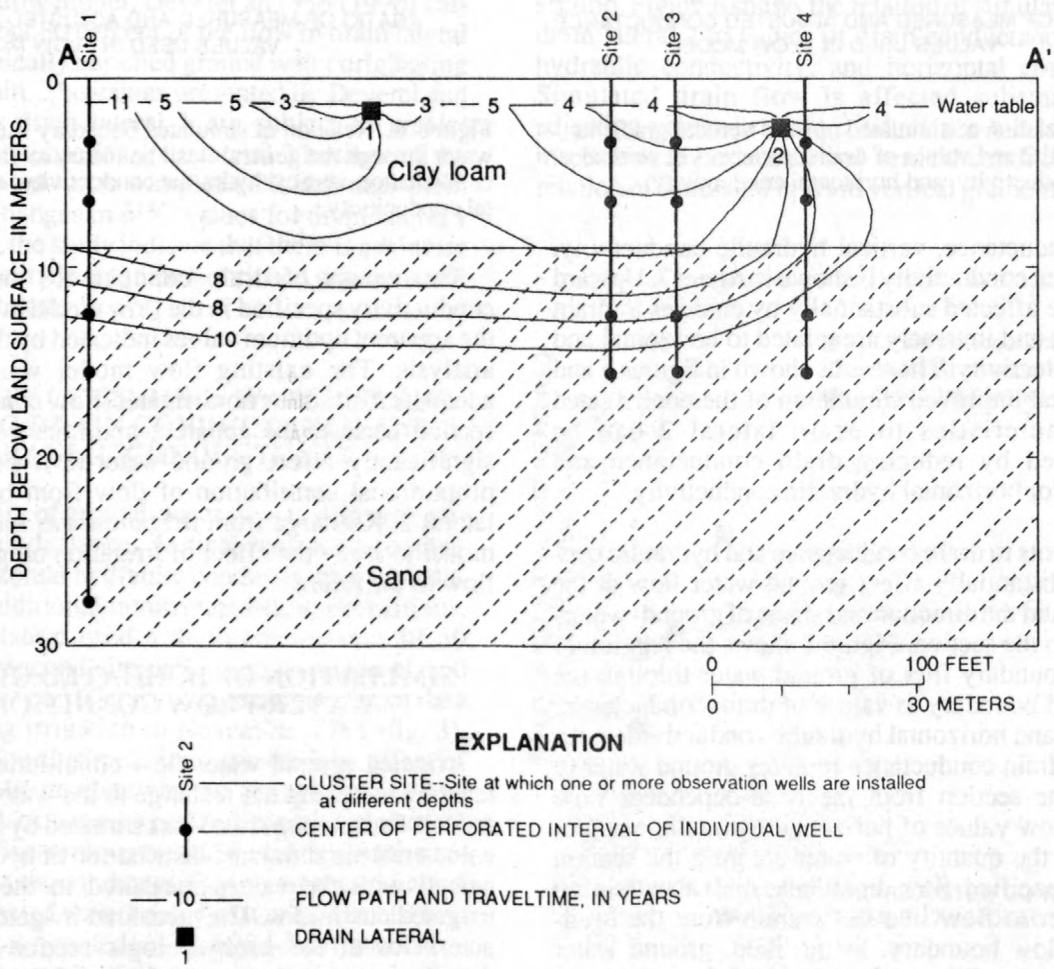

Figure 9. Simulated ground-water-flow paths and estimated traveltimes for irrigated conditions. Simulated flow for drain lateral 1 is 27 $(m^3/yr)/m$; drain lateral 2 is 63 $(m^3/yr)/m$.

Table 2. Proportion of simulated flow in the drain laterals from upward flow of water at depths greater than 6 meters and calculated selenium loads for the ground-water-flow simulations

Recharge rate (m/yr)	Drain lateral 1					Drain lateral 2				
	Simulated discharge [(m^3/yr)/m]	Flow from beneath [(m^3/yr)/m]	Proportion from beneath (percent)	Selenium load from beneath [(kg/yr)/m]	Selenium load [(kg/yr)/m]	Simulated discharge [(m^3/yr)/m]	Flow from beneath [(m^3/yr)/m]	Proportion from beneath (percent)	Selenium load from beneath [(kg/yr)/m]	Selenium load [(kg/yr)/m]
0.0	4	2	50	1.6	2.1	46	32	69	25.0	28.4
.16	10	4	40	3.1	4.6	52	31	59	24.2	29.3
.41	19	6	32	4.7	7.9	62	28	45	21.8	30.1
.59	27	7	26	5.5	10.4	68	29	43	22.6	32.2
1.0	43	9	21	7.0	15.3	84	28	33	21.8	35.5

from depths greater than 6 m to the drain laterals for recharge rates of 0.0, 0.16, 0.41, 0.59, and 1.0 m/yr are shown in table 2. The model results indicate that recharge from irrigation increases the horizontal and vertical gradients to the drain laterals and consequently increases drain flow. The model results further indicate that the quantity of water flowing upward from beneath drain lateral 1 increases with increasing recharge; whereas the upward flow to drain lateral 2 from depths greater than 6 m remains relatively constant. Increased ground-water flow from areas above and adjacent to the drain laterals decreases the proportional contribution of water from depths greater than 6 m. The composition of drain-lateral water and drain-lateral selenium loads is affected by the mixing of relatively high quality water at depths less than 6 m and low quality water from depths greater than 6 m.

SELENIUM LOADS IN DRAIN LATERALS

The concentrations of selenium in ground water at depths adjacent to the drain laterals and at depths greater than 6 m were estimated from the median concentrations of selenium in ground-water samples collected in the 3- and 6-meter wells (245 µg/L) and 12-, 15-, and 27-meter wells (780 µg/L), respectively. The selenium loads estimated from the ground-water-flow simulations are shown in table 2. The relation of logs of selenium loads and drain-lateral flows is shown in figure 10. There is general agreement between the measured and simulated results. The simulated loads in drain lateral 1 are high relative to measured values indicating that selenium concentrations in ground water adjacent to and beneath drain lateral 1 probably are lower than 245 and 780 µg/L, respectively. The simulated contribution of ground water adjacent to drain lateral 2 to selenium loads in the drain are smaller than the measured values, and selenium concentrations adjacent to drain lateral 2 probably are larger than 245 µg/L. Selenium concentrations in ground-water samples collected next to drain lateral 2 are about 900 µg/L (Deverel and Fio, 1990, fig. 10).

The ground-water-flow model seems to accurately simulate the contribution of ground water from areas around the drain laterals. Selenium loads increase with increasing rate of recharge and drain flow, but the proportional contribution of high-selenium water from depths greater than 6 m decreases due to dilution by water from depths less than 6 m.

Isotopic enrichment and high selenium concentrations in ground water in this field and the simulated flow paths shown in figures 5 and 9 indicate that

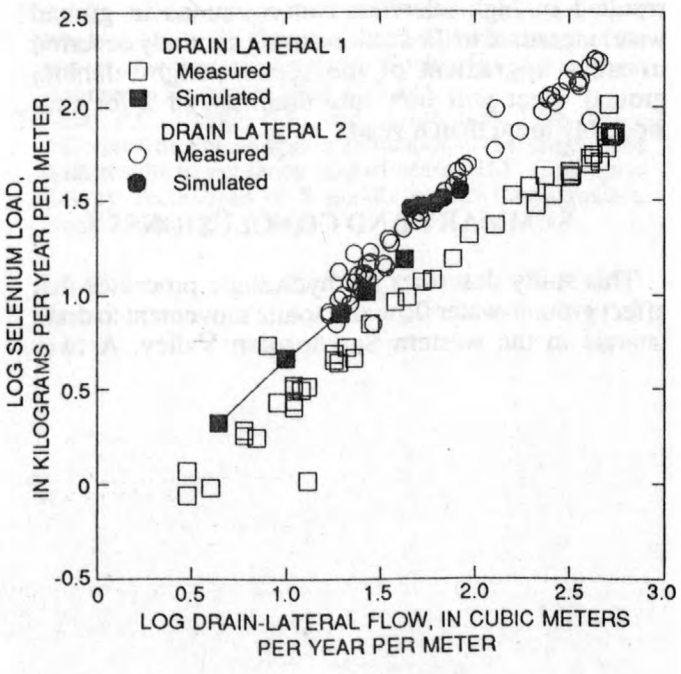

Figure 10. Relation of logs of measured and simulated selenium loads in drain laterals 1 and 2.

enriched ground water originally near the land surface has been displaced downward into the sand layer underlying this field. The simulation results presented in this paper and the geochemical assessment presented in Deverel and Fio (1990) indicate that the high-selenium ground water will flow to drain lateral 2 for several years. Traveltimes for the irrigated and nonirrigated flow paths originating in the sand layer at the upgradient boundary of the section are greater than or equal to 8 years. The estimated traveltimes are substantially less than the 19 years that the field was drained at the time of this study (1988). Ground water at depths greater than 6 m in this field at the time the drainage system was installed already should have flowed into drain lateral 2, thus additional high-selenium ground water has probably moved into the section from areas upgradient of the field. The high-selenium ground water flowing into the section in the sand layer and its estimated traveltime of at least 8 years to reach drain lateral 2 indicate that high concentrations of selenium in the discharge from drain lateral 2 will continue for a minimum of 8 years following this study.

The two-dimensional approach taken here, however, is limited in simulating ground-water flow and solute movement to the drain laterals because it does not account for flow to the drain laterals from areas upgradient of the geohydrologic section; moreover, there is no data for ground-water selenium concentrations upgradient of the section. If the processes that have resulted in high-selenium concentrations in ground water measured in the section during the study occurred in areas upgradient of the section, high-selenium ground water will flow into drain lateral 2 for considerably more than 8 years.

SUMMARY AND CONCLUSIONS

This study describes the hydrologic processes that affect ground-water flow and solute movement to drain laterals in the western San Joaquin Valley. A two-dimensional ground-water-flow model in conjunction with geochemical and hydrologic data was used to quantitatively assess these hydrologic processes. The model simulates steady-state ground-water flow and advective solute movement under nonirrigated and irrigated conditions.

Simulated ground-water-flow paths during nonirrigated conditions (no recharge) generally are horizontal except near the drain laterals. Irrigated flow paths (nonzero recharge) are deep and concentric in clay loam and horizontal in sand underneath the clay loam at 9 m below land surface. Simulations of irrigated and nonirrigated flow conditions indicate that ground water moves from the sand layer to a drain lateral 2.7 m below land surface (drain lateral 2).

The ground-water-flow simulations of nonirrigated conditions indicate that about 89 percent of the flow in drain lateral 2 is deep ground water originating at depths greater than 6 m below land surface. Simulation of irrigated conditions indicates that the proportion of deep ground water entering drain lateral 2 decreases with increasing recharge. The proportions of deep ground-water flow entering the drain laterals simulated by the model are in general agreement with geochemical data measured in the field.

Selenium loads in drain laterals calculated by the ground-water-flow model for different drain flows are in general agreement with the measured values. Selenium loads in drain laterals increase with increasing drain flow and increasing recharge. Traveltimes calculated during this study and the distribution of selenium concentrations in ground water indicate that drain lateral 2 may continue to collect high-selenium ground water for more than 8 years.

REFERENCES CITED

Belitz, Kenneth, and Heimes, F.J., 1990, Character and evolution of the ground-water flow system in the central part of the western San Joaquin Valley, California: U.S. Geological Survey Water-Supply Paper 2348, 28 p.

Bouwer, H., 1978, Groundwater hydrology: New York, McGraw-Hill Book Company, 480 p.

Cooper, H.H., Jr., Bredehoeft, J.D., and Papadopulos, I.S., 1967, Response of a finite-diameter well to an instantaneous charge of water: Water Resources Research, v. 3, no. 1, p. 263-269.

Deverel, S.J., and Fio, J.L., 1990, Ground-water flow and solute movement to drain laterals, western San Joaquin Valley, California. I. Geochemical assessment: U.S. Geological Survey Open-File Report 90-136, 23 p.

Deverel, S.J., and Fujii, Roger, 1988, Processes affecting the distribution of selenium in shallow groundwater of agricultural areas, western San Joaquin Valley, California: Water Resources Research, v. 24, no. 4, p. 516-524.

Deverel, S.J., and Gallanthine, S.K., 1989, Relation of salinity and selenium in shallow groundwater to hydrologic and geochemical processes, western San Joaquin Valley, California: Journal of Hydrology, v. 109, p. 125-149.

Hvorslev, M.J., 1951, Time lag and soil permeability in groundwater observations: Vicksburg, Mississippi, U.S. Army Corps of Engineers Experimentation Station, Bulletin 36, 50 p.

Johnson, A.I., Moston, R.P., and Morris, D.A., 1968, Physical and hydrologic properties of water-bearing deposits in subsiding areas in central California: U.S. Geological Survey Professional Paper 497-A, 71 p.

Jury, W.A., 1975a, Solute traveltime estimates for tile drained fields, I, Theory: Soil Science Society of America, v. 39, p. 1020-1024.

——1975b, Solute traveltime estimates for tile drained fields, II, Experimental: Soil Science Society of America, v. 39, p. 1024-1028.

Kirkham, D., 1949, Flow of ponded water into drain tubes in soil overlying an impervious layer: Transactions American Geophysical Union, v. 30, no. 3, p. 369-385.

Kirkham, D., 1958, Seepage of steady rainfall through soil into drains: Transactions American Geophysical Union, v. 39, no. 5, p. 892-908.

Luthin, J.N., Fernandez, P., Maslov, B., Woerner, J., and Robinson, F., 1969, Displacement front under ponded leaching: Journal of the Irrigation and Drainage Division, Proceedings of the American Society of Civil Engineers, v. 95, p. 117-125.

McDonald, M.G., and Harbaugh, A.W., 1988, A modular three-dimensional finite-difference ground-water flow model: U.S. Geological Survey Techniques of Water-Resources Investigations, Book 6, Chap. A1, 586 p.

Ortiz, J., and Luthin, J.N., 1970, Movement of salts in ponded anisotropic soils: Journal of the Irrigation and Drainage Division, Proceedings of the American Society of Civil Engineers, v. 96, p. 257-263.

Pickens, J.F., Gillham, R.W., Cameron, D.R., 1979, Finite-element analysis of the transport of water and solutes in tile-drained soils: Journal of Hydrology, v. 40, p. 243-264.

Pollock, D.W., 1988, Semianalytical computation of path lines for finite-difference models: Ground Water, v. 26, p. 743-750.

——1989, Documentation of computer programs to compute and display pathlines using results from the USGS modular three-dimensional finite-difference ground-water flow model: U.S. Geological Survey Open-File Report 89-381, 110 p.

Reilly, T.E., Franke, O.L., Buxton, H.T., and Bennett, G.D., 1987, A conceptual framework for ground-water solute-transport studies with emphasis on physical mechanisms of solute movement: U.S. Geological Survey Water-Resources Investigations Report 87-4191, 44 p.

Tod, I.C., and Grismer, M.E., 1988, Drainage efficiency and cracking clay soil: Paper no. 88-2588, Proceedings of the winter meeting of American Society of Agricultural Engineers, December 1988, Chicago.

Trescott, P.C., Pinder, G.F., and Larson, S.P., 1976, Finite difference model for aquifer simulation in two dimensions with results of numerical experiments: U.S. Geological Survey Techniques of Water-Resources Investigations, Book 7, Chap. C1, 116 p.

GPO 787-982/39217

POSTAGE AND FEES PAID
U.S. DEPARTMENT OF THE INTERIOR
INT 413

U.S. DEPARTMENT OF THE INTERIOR
Geological Survey, Room W-2234
2800 Cottage Way, Federal Building
Sacramento, CA 95825

OFFICIAL BUSINESS
PENALTY FOR PRIVATE USE $300
SPECIAL 4TH CLASS BOOK RATE